Some Physical and Chemical Properties of the Arctic Winter Aerosol in Northeastern Canada

W. R. LEAITCH, R. M. HOFF AND S. MELNICHUK

Atmospheric Environment Service, Downsview, Ontario M3H 5T4, Canada

A. W. HOGAN

Atmospheric Sciences Research Center, State University of New York at Albany, Albany, NY 12222

(Manuscript received 16 April 1983, in final form 23 March 1984)

ABSTRACT

Measurements spanning much of the particle size spectrum were made on the surface aerosol arriving at Igloolik, Northwest Territories, Canada during late February 1982. Vertical profiles of aerosol particle concentration were obtained during one day of the study period. Concentrations of Aitken nuclei and cloud condensation nuclei as well as the aerosol light-scattering coefficient were measured instrumentally several times a day. Inertial impaction systems were used to separate and collect particles for microscopic sizing and chemical analysis. Suspended and precipitating ice crystals were inertially collected on microscope slides. The aerosol observations were accompanied by observations of temperature, wind speed and direction, visibility and cloud type. An upper-air station at Hall Beach, <100 km from Igloolik, provided radiosonde data.

Diurnal variations in the Aitken nucleus concentrations were observed on several clear days. The concentrations were frequently seen to follow the diurnal temperature variation, reaching a maximum near midday. Vertical profiles of Aitken nucleus concentrations obtained prior to and during one of these diurnal peaks suggests that this pattern was limited to the near-surface layer. Throughout the study, virtually all of the aerosol particle mass lay between 0.2 and 4.0 μm diameter. There was little indication of any diurnal change in the particle concentration in this size range. A clear difference in the quality of the air reaching Igloolik was detected on 23 February. Associated with this was a doubling of the particle concentration while the apparent particulate mass increased from ~6 to ~11 $\mu g\ m^{-3}$. Impacted aerosol particles were found to be composed of 15–50% water soluble compounds before 23 February and 40–100% after this date. Sulfate was the dominant ionic species in all cases. Vertical profiles of the large aerosol particles, obtained with an airborne nephelometer, suggested a slightly enhanced concentration at the surface and a uniform concentration in the lower troposphere. Profiles of Aitken nucleus concentrations pointed to a surface source of small nuclei which diffused vertically and independently of the larger particles.

Suspended ice crystals may have accounted for a significant portion of the degradation in visibility observed throughout the study.

1. Introduction

The Arctic is a sink region for heat, water vapor and particulate material which are all transported there meteorologically. High pressure systems develop as this air assumes arctic properties; Megaw and Flyger (1973) hypothesized that global background aerosol might be found in these air masses during summer while the air would be polluted in the winter. Indeed, during winter and spring, greater aerosol mass (e.g., Rahn *et al.*, 1977; Barrie *et al.*, 1981) and number concentrations (e.g., Radke *et al.*, 1976; Heintzenberg, 1980) are measured at the surface than in summer. Many hypotheses have been presented (Rahn, 1982) to show how the increase in aerosol and gases in the winter accompanies the advection of midlatitude air into the arctic basin.

These transport ideas have to date been formulated from surface observations of collected aerosol material, light-scattering parameters and Aitken nuclei from several locations in the Arctic. The last two measurements are capable of resolving short term variations in aerosol concentration, but filter or impactor collections require several days to gather sufficient material for analysis and cannot reflect mesoscale changes in aerosol content. Vertical profiles are necessary to determine if these variations are due to inhomogeneity within the air mass, or to variations in the mixing of air which is enhanced or depleted in particles at the surface.

Arctic visibilities are often near the Rayleigh limit in summer, and are only disturbed by looming and mirage. Winter visibility is generally quite poor in the Arctic basin and was the subject of some studies (e.g., Mitchell, 1957) during the periods of extensive Arctic air operations which followed World War II. Since then it has been suggested that aerosol advected from midlatitudes, together with ice crystals, may be re-

sponsible for the increase in turbidity observed in winter (Shaw, 1975; Shaw and Stamnes, 1980).

This paper discusses the results of quantities measured at the surface and from an aircraft, enabling the near-surface Arctic aerosol to be described in some detail over much of its size spectrum. Based upon these results, inferences are drawn on the source and recent history of the aerosol.

2. Site and observations

The experiments were conducted at or in the vicinity of the Eastern Arctic Research Laboratory on Igloolik Island, in the Foxe Basin (see Fig. 1), during the latter part of February 1982. Igloolik Island is a low island with a maximum elevation of ~60 m above sea level and about 6 × 10 km maximum dimensions. A settlement of about 800 people surrounds the laboratory, at the head of a small bay on the southeast side of the island. The most frequent surface wind during winter is from the west to north-northwest at 10–25 km h^{-1}. Winds which preceed or accompany precipitation are frequently from easterly directions.

Measurements of Aitken nuclei (AN) were made with a modified Gardner (Rich, 1955) counter, described by Hogan *et al.* (1975), from 13 through 27 February. This instrument will resolve changes of ±10 cm^{-3} in a total concentration of 25 cm^{-3}. Observations were taken a few meters upwind of the westernmost building of the settlement, depending on the wind direction.

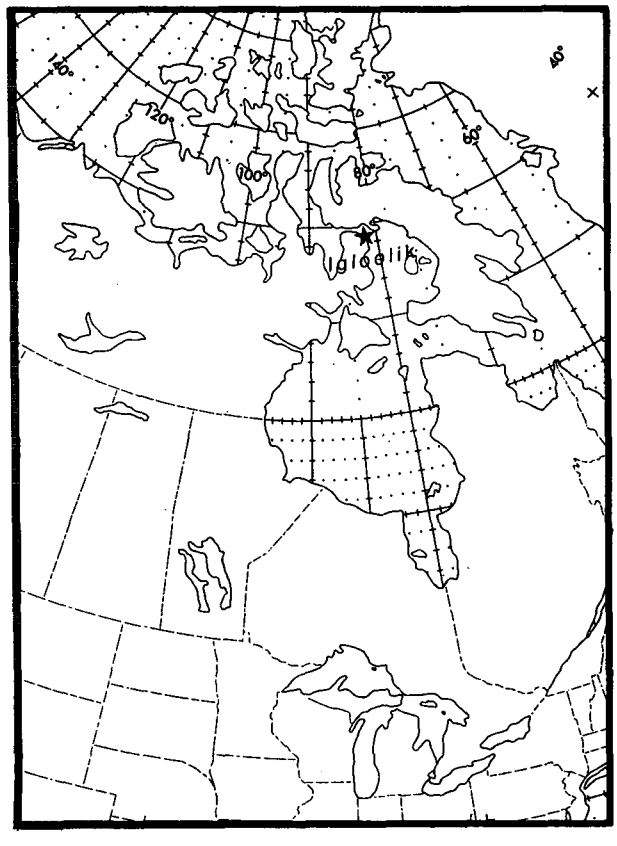

FIG. 1. Location of Igloolik, Northwest Territories, Canada.

Aerosol particles were collected with filters (teflon) and Andersen (Andersen Samplers Inc., Atlanta, Georgia) cascade impactors (polyethylene substrates) and analyzed for concentrations of the water soluble ions, Na^+, K^+, NH_4^+, Ca^{++}, Mg^{++}, Cl^-, NO_3^- and $SO_4^=$. Collectors were exposed every 48 hours at the highest point on the island, about 2 km north-northwest of the settlement. This site has been described elsewhere (Barrie *et al.*, 1981). A parallel set of impactor collections as well as instrumental measurements of cloud condensation nuclei (CCN), bulk light scattering coefficient and individual particle scattering were made at the laboratory from an inlet about 12 m above ground level.

Particle concentrations in the size range between 0.4 and 3.0 μm diameter were determined using a Royco (Royco Instruments, Menlo Park, California) 225 optical particle counter. This instrument was calibrated after the experiment with polystyrene latex spheres. Microscopic measurements of the concentrations of particles larger than about 0.6 μm were performed on aerosol samples collected on slides in a May impactor (May, 1945). Observations of the CCN spectrum between 0.15 and 0.04% supersaturation with respect to water were done using a version of the diffusion tube described by Leaitch and Megaw (1982a). Calibrations of this instrument were performed both before and after the study with monodisperse NaCl particles. A MRI (Meteorology Research Inc., Altadena, California) model 1550 integrating nephelometer was used to measure the light-scattering coefficient b_{scat} of the ambient aerosol particles. The inlet to the nephelometer was heated to provide a nearly dry aerosol to the instrument and a calibration with Freon 12 was performed just prior to the study.

Northwest winds were frequently encountered and caused passage of the air over two houses before reaching the laboratory. The sampling lines were elevated between 3 and 4 m above the house chimneys. Intermittent plumes from the chimneys were continually observed to descend beneath the house roofs. The plumes passed well below the sampling lines and there were no indications that the output from these chimneys was being detected in the measurements of CCN or with the Royco. Further, a comparison of 48-hour impactor samples collected concurrently at the lab and at the ridge, from 19 to 26 February, showed no large difference in the concentration of major water soluble ions. In fact, the total concentration of these ions was determined to be ~24% greater at the ridge site as compared to the laboratory. This discrepancy is within the error of measurement. As the ridge is located north of the settlement and was not subject to local pollution

sources during the study, it was concluded that the village had a negligible effect on our laboratory measurements.

Visual range observations were made at the time of daytime AN measurements by observing landmarks against the horizon. Since there are many uncertainties in this procedure, particularly when snow cover reduces the contrast, these deduced visual ranges must be regarded only as estimates. By the same token they are directly comparable in so much as the same observer utilized the same visual references on each occasion. The results for the study period, shown in Fig. 2, ranged between 10 and 60 km, in the absence of visible precipitation.

Even when precipitation was not visible, small ice crystals were observed suspended in the air during periods of twilight and darkness by flashing a photographic strobe light toward the northern sky. No optical effects attributable to these crystals were apparent during sunlit hours; however, ice crystal replicas collected during these times substantiated their presence throughout the study.

Formvar ice crystal replicas (Schaefer, 1946) were collected several times a day on 25 × 75 mm slides, by swinging them across the wind at arm's length. This method is fairly efficient for impacting crystals with dimensions > 100 μm, but is ineffective for crystal sizes < 30 μm.

A deHaviland Twin Otter aircraft was chartered to make observations of vertical variations in the light-scattering coefficient and the AN concentration. The aircraft was equipped with a forward facing nearly isokinetic probe mounted in an aluminum panel replacing the copilot's window, such that the sampling intake was ahead of the propeller line. About 1.5 m of flexible tubing carried air to the nucleus counter and to a second MRI integrating nephelometer. Air temperature and pressure were recorded from a thermistor bead and a Rosemount capacitive pressure transducer at the tip of the inlet. This nephelometer was also calibrated against Freon 12 prior to and after the series of flights.

Three flights were made on 26 February, just after sunrise, just before sunset and in the evening over the sampling site and the adjacent Foxe Basin.

3. Results of surface measurements

A chronology of meteorological parameters (wind direction, temperature and visibility estimate) and particle concentrations are plotted in Figs. 2 and 3. During the period 14–17 February winds were light from the north through west sector. The sky was cloudless but there was considerable dispersion of light. A distinct diurnal variation was observed in the AN concentrations (Fig. 2) during this time period. The maximum concentration occurred between 1200 and 1800 LST, which usually coincided with the time of the maximum daily surface air temperature.

The wind direction shifted to southeasterly and wind speed increased on 18 February, accompanied by snowfall. Inclement weather limited Aitken nuclei measurements to a single observation during this time, although ice crystal and other meteorological parameters were continuously observed. Precipitation ceased early on 19 February, and by noon light northwest winds were re-established. This situation continued until early on 21 February when the surface wind speed diminished. A period of thickening cirrus overcast and a light snowfall occurred on the night of 21 February.

Northwest winds of 10–25 km h^{-1} began on 22 February and continued to the end of the study on 27 February. Diurnal variations in AN concentrations consistent with those observed on 14–17 February were also found on 24 and 26 February, with the maximum concentration again coincident with small temperature increases at the surface. The concentration of particles greater than about 0.6 μm (Fig. 3) for the period 21–27 February does not suggest a diurnal variation in the concentration of these particles.

Cloud condensation nucleus spectra and the aerosol particle size distributions, obtained from the Royco measurements, were made in sequence from 21 to 26 February inclusive. Averages of the results are plotted together in Figs. 4a and b representing observations prior to and after a distinctive change in air quality late on 22 February, respectively. The cumulative size distributions have been extrapolated below 0.6 μm based on coincident observations of AN and CCN concentrations as b_{scat}. Also shown in Fig. 4b is the result of light microscope measurements of the particle size distributions for 23–26 February. This curve possesses a slope very close to that obtained from the Royco measurements, but is about a factor of 3 lower in absolute concentration.

The mean value of b_{scat} for 21–22 February was determined to be 2.5×10^{-5} m^{-1}. This signal increases very sharply, as seen in Fig. 3, at or about 2400 LST 22 February. From then until 27 February the mean b_{scat} value was 4.3×10^{-5} m^{-1}.

Results of the major water-soluble ion analyses of the multistage impactor samples are illustrated in Figs. 5 and 6. Superimposed in these figures are the total particle mass and surface distributions derived from the number distributions (Fig. 4) assuming spherical particles with a mass density of 2.0 g cm^{-3}. The cutoff for the backup filter has arbitrarily been set to 0.2 μm in order to agree with measurements of the number distributions. The sizes of the impacted aerosol particles may have been slightly overestimated due to particle deliquescence at high relative humidities (surface relative humidity ranged from 60 to 80%) but particle bounce-off upstream in the impactor may alternatively have biased the mass distribution to smaller sizes.

Figures 5 and 6 also show the mass distributions derived from the CCN measurements by comparison with the particle number distribution and assumption

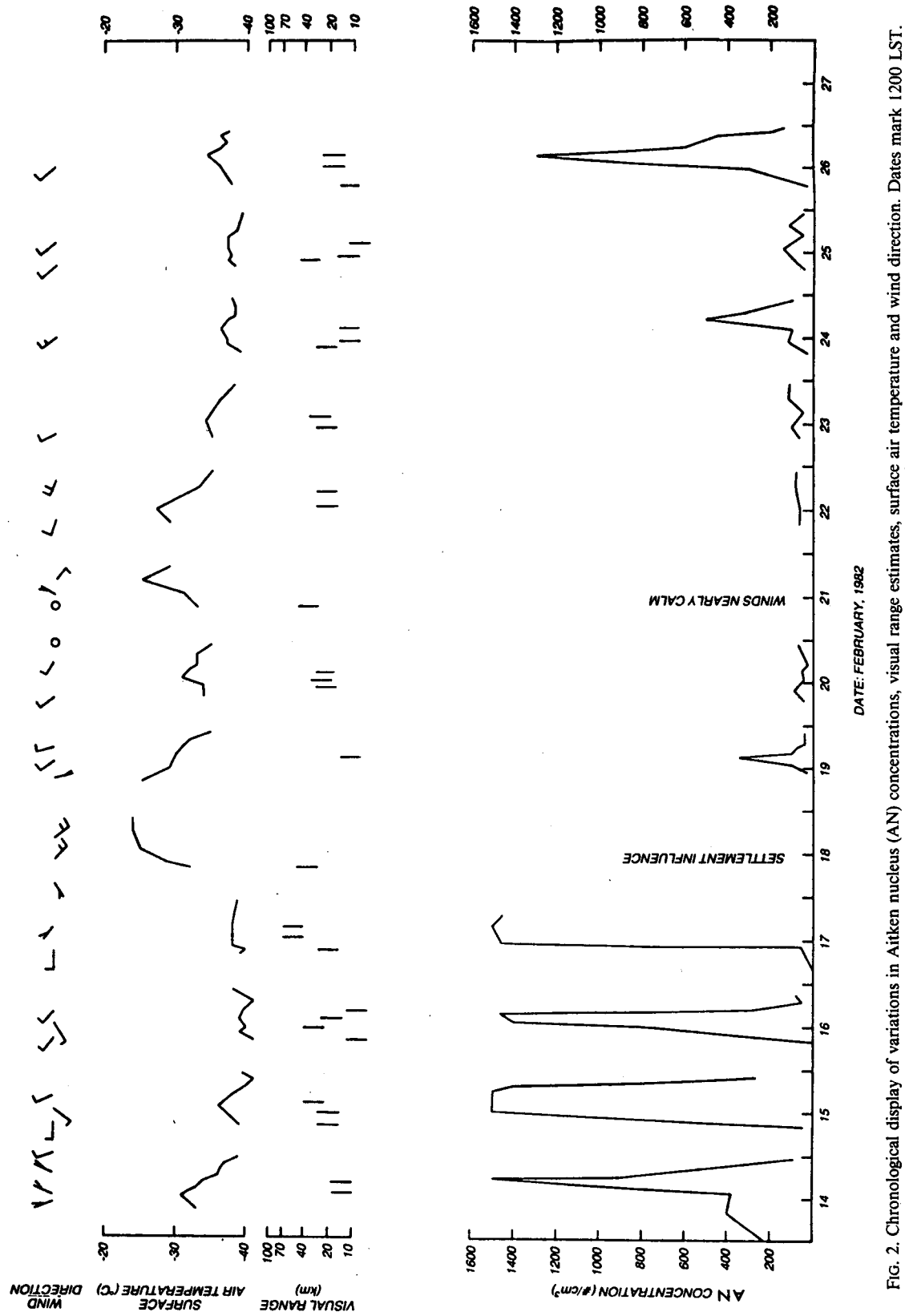

FIG. 2. Chronological display of variations in Aitken nucleus (AN) concentrations, visual range estimates, surface air temperature and wind direction. Dates mark 1200 LST.

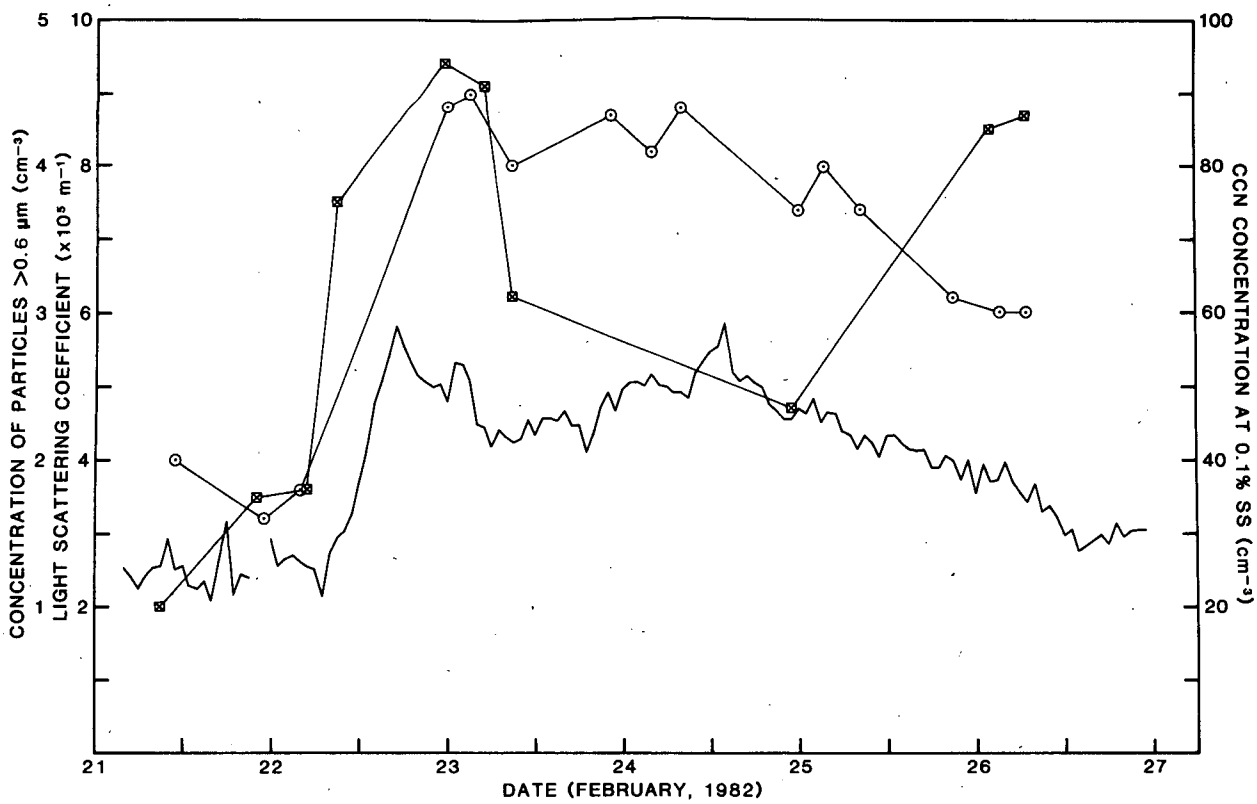

FIG. 3. Chronological variation of concentrations of CCN active at 0.1% supersaturation (squares), concentration of large particles > 0.6 μm (circles) and hourly averaged particle light scattering coefficient (unmarked curve). Dates mark 1200 LST.

of $(NH_4)_2SO_4$ as the water soluble component of the nuclei. This derivation has been discussed by Leaitch and Megaw (1982b) and gives an approximate indication of the distribution of the water soluble mass in the submicron-sized particles. The accuracy of this approach is in large part determined by the accuracy of the evaluation of the supersaturation. In the case of these measurements, this is best for supersaturation in excess of ~0.07%, corresponding to particles < 0.4 μm diameter.

The smallest ice crystals collected during the study were about 10 μm in the smallest dimension. Smaller crystals may have been present (in the air), but were not collected. Concentrations were estimated at between 3 and 30 per liter. Microscopic examination of the crystal replicas showed them to most frequently be of the column, long column or thick plate type, followed by thin plates or asymmetrical plates. Fragments of the primary crystals indicated re-entrainment by the wind, even though blowing snow was not apparent over the extremely dense firn which covered the surface.

Little information has been published on the scattering (as opposed to refraction) of light by ambient ice crystals, but the cross-sectional area of a crystal must bear some relation to the amount of light it will scatter. Thus, an attempt was made to estimate this area from the replica dimensions, measured with a Porton eyepiece graticule. During 14–16 February, crystal replicas were obtained within 30 minutes of each observation of the visual range. For this period the visual range estimates have been plotted as a function of total ice crystal cross-sectional area per unit volume. The result, shown in Fig. 7, suggests that the reduced visibility was some consequence of the suspended ice crystals.

4. Results of aircraft measurements

Vertical profiles of the light-scattering coefficient, AN concentration and temperature were made on three separate flights over Igloolik and the Foxe Basin on 26 February. Aitken particle concentration was not measured on the final flight. Radiosonde data from the Hall Beach (<100 km distant) upper-air station for 0700 LST (1200 GMT) are shown in Fig. 8. The temperature profile is isothermal for 1 km above a surface inversion. During the period from 1900 LST 24 February to 0700 26 February, the isothermal layer from 1 to 2 km almost completely decoupled the upper tropospheric flow (above 600 mb) which was southerly, from the northerly surface flow (below 800 mb). The surface winds were moderate and the isothermal layer nearly calm.

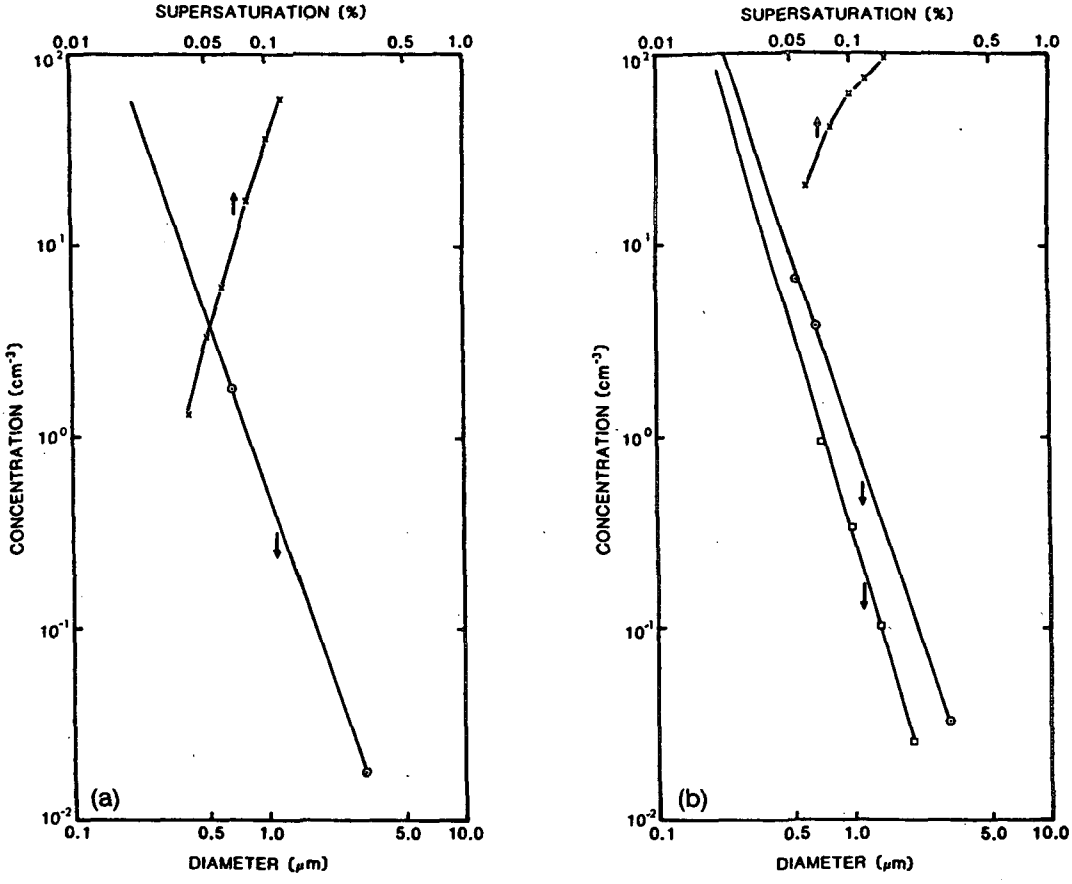

FIG. 4. CCN spectra and cumulative particle number distribution (circles, Royco; squares, light microscope) for (a) 21–22 February 1982 and (b) 23–26 February.

Results of the ascent and descent portions of each flight are shown in Fig. 9. The nephelometer trace (solid line) has been corrected for pressure variations and Rayleigh scattering, and averaged over every 30 m in altitude. The error bars indicate the rms fluctuation in the raw data before smoothing.

The morning ascent (Fig. 9a) over Igloolik showed an AN concentration of 120 cm^{-3} at 100 m above the surface, decreasing to <50 cm^{-3} for the remainder of the ascent. A large area of open water was observed from the top of the ascent (3 km), northeast of Igloolik in an area of the Foxe Basin noted for year-round open water (Fury and Hecla Straights). Arctic sea-smoke was seen at the upwind edge of a path of "open" (i.e., 6 octas of ice cover) water. A descent (Fig. 9b) was made to 30 m above this water surface. The AN concentration increased to 60–80 cm^{-3} at the top of this smoke layer and reached 350 cm^{-3} at 30 m. On both segments of this flight the nephelometer readings were indistinguishable from Rayleigh scattering above 1400 m. Below this, b_{scat} increased gradually. Some slight increase in b_{scat} was noted beneath the top of the inversion which was located at ~1000 m. The maximum value of the coefficient was recorded near the surface, in the smoke layer. On the return to Igloolik the AN concentration was 200 cm^{-3} at 200 m.

The afternoon flight (Figs. 9c and d; note scale change) followed a similar flight path as that in the morning. Aitken nuclei concentrations in the sea smoke were again widely variable, but much higher, ranging from 750 to 3000 cm^{-3}. Concentrations of 100–300 cm^{-3} were measured 100 m above the ice surface on the return leg. Profiles of the b_{scat} were relatively uniform up to the inversion, which had lowered to between 600 and 800 m. Above this level they were again indistinguishable from Rayleigh scattering.

The final flight of the day took place in the evening from 1900 to 2015 LST over Hall Beach (Figs. 9e and f). No significant differences were observed in either the temperature or light-scattering coefficient profiles.

Surface concentration of AN on this day were ~50 cm^{-3} about an hour before the morning flight. By 1200 LST they had increased to 300 cm^{-3} and at 1500, prior to the second flight, the concentration reached a peak of 1300 cm^{-3}. Concentrations decreased after this to 600 cm^{-3} at 1700 and had diminished further to 180 cm^{-3} by 2200.

Measurements of CCN at the surface indicated the

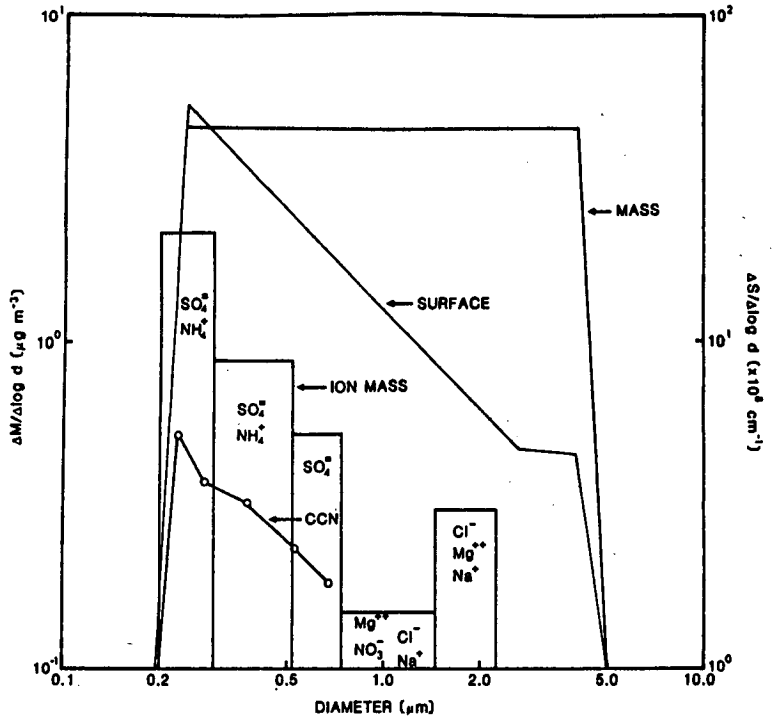

FIG. 5. Particle mass (assuming spherical particles with a density of 2.0 g cm^{-3}) and surface distributions based on Royco measurements. Also shown is the major ion distribution determined from multistage impaction analysis and the water soluble mass distribution derived from the CCN measurements. The Royco and CCN results are for 21–22 February. The ion measurements are for 19–21 February.

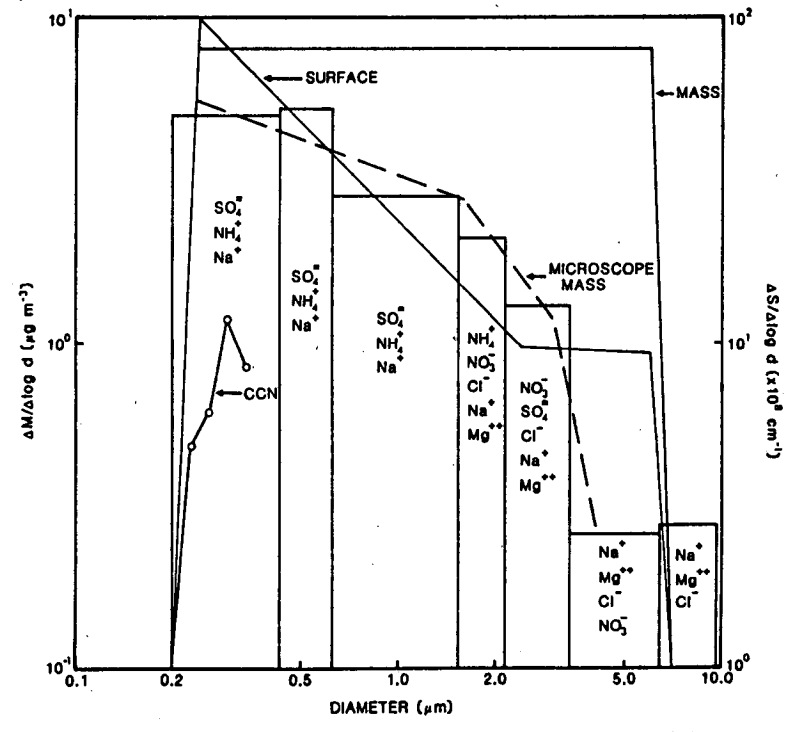

FIG. 6. As in Fig. 5 but for 23–26 February. Also included is the particle mass (density of 2.0 g cm^{-3}) distribution determined from the microscope measurements.

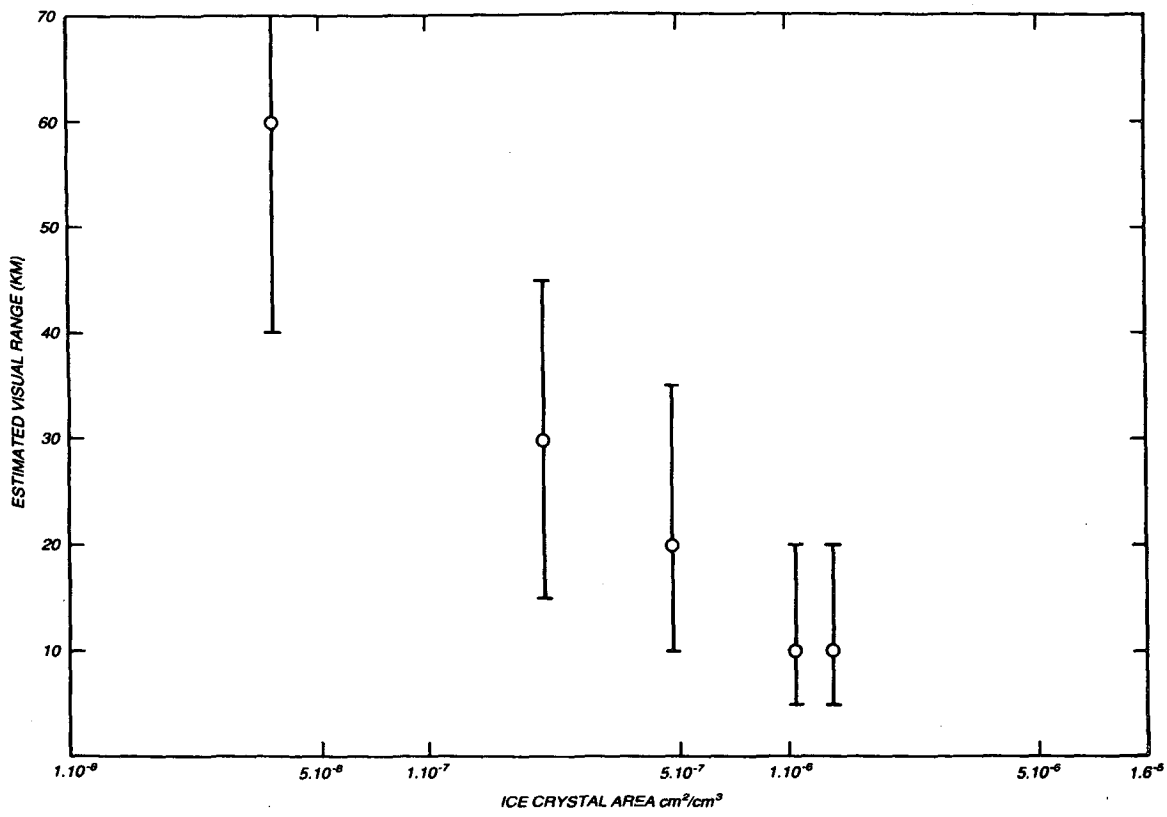

FIG. 7. Total ice crystal area per unit volume versus estimated visual range.

presence of more nuclei active at supersaturations above 0.1% than on previous days, but no change was observed for lower supersaturations. Correspondingly, the concentration of large particles determined with the Royco did not deviate significantly from the mean concentration for the period 23–26 February, and the

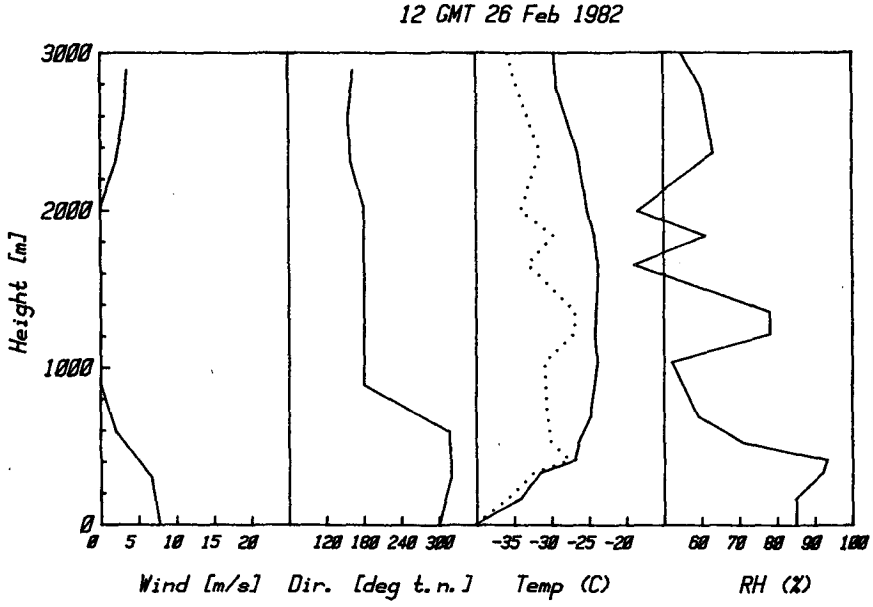

FIG. 8. Vertical temperature and wind structure of lower troposphere from Hall Beach radiosonde release at 0700 LST 26 February. Dew point temperature is shown as a dotted line.

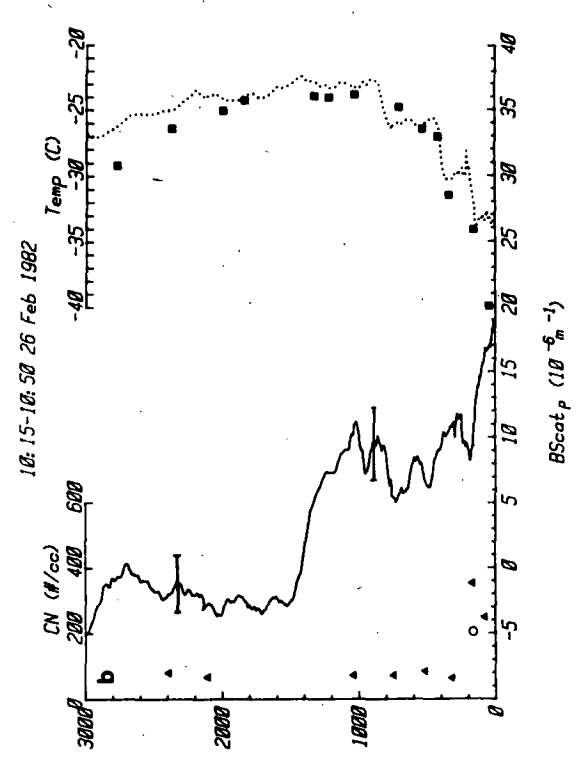

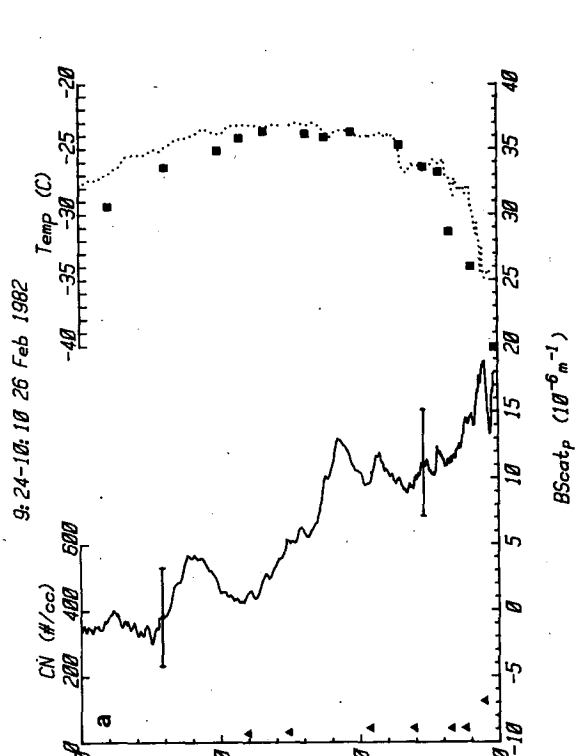

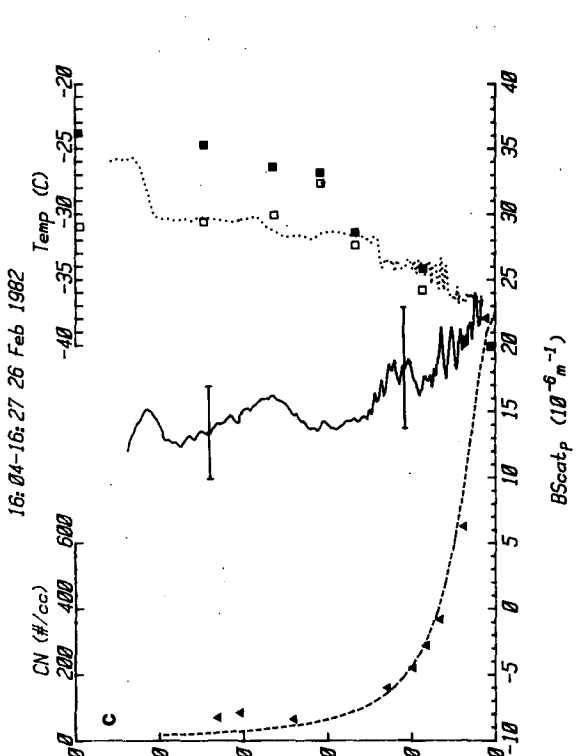

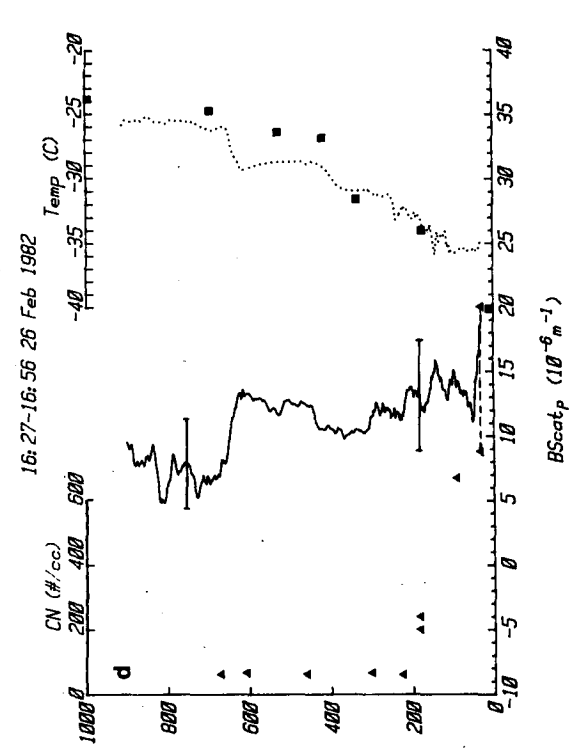

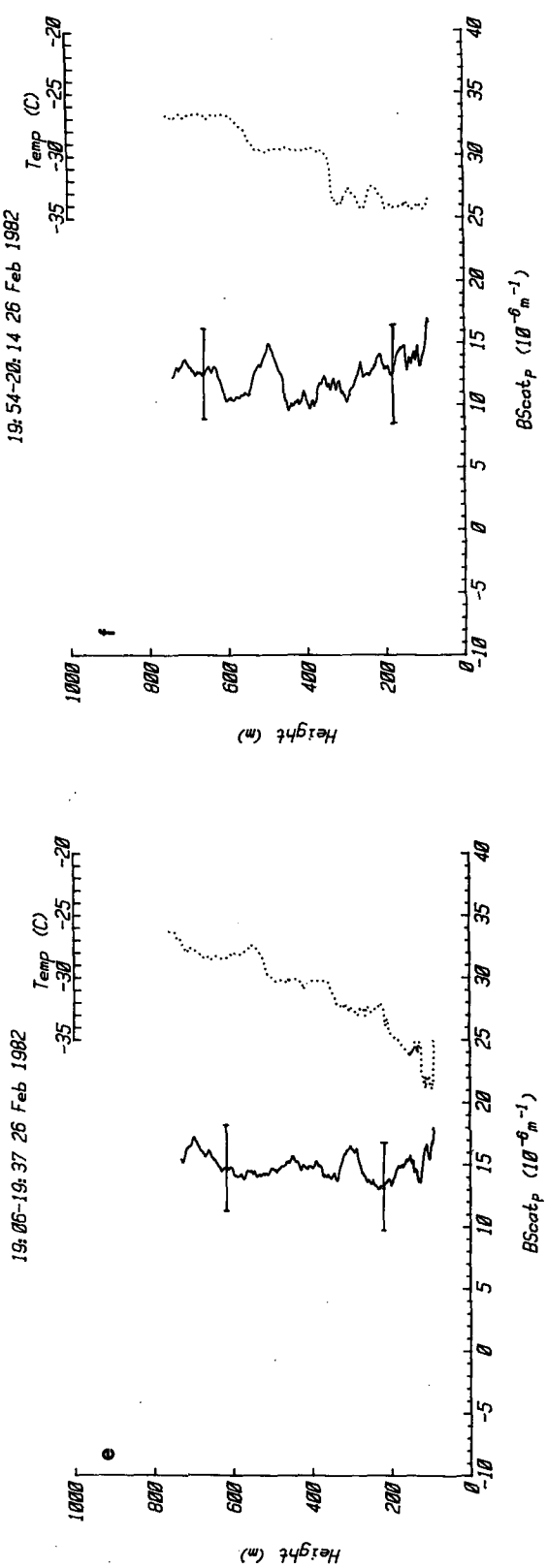

FIG. 9. Flight results for 26 February for the times indicated (LST). Shown are the values for b_{scat} (solid curve), AN concentrations (triangles), aircraft temperature (dotted curve), 0700 radiosonde temperature (solid squares) and radiosonde dew point temperature (open squares).

surface light scattering signal gave no indication of any diurnal variation.

5. Discussion

Diurnal variations in AN concentrations are believed to have resulted from small particle production via gas-to-particle reactions occurring during daylight hours. Subsequent coagulation with larger members of the size spectrum (Hogan, 1977) returned the concentration to original levels. Observations from vertical profiles indicate that this production was probably a surface based phenomenon and not a consequence of atmospheric motion. It can be shown that these small particles contributed little to the total mass of aerosol particles and scattering of light. Summer observations of particle size using diffusion batteries at Igloolik and Barrow, Alaska (Hogan *et al.*, 1982) have indicated that particles associated with diurnal peaks in AN concentrations are typically about 0.02 μm or smaller. The mutual coagulation of 10^3 particles of this size would contribute only one particle $\sim$ 0.2 μm in diameter. In general, the effect on these measurements would be negligible, particularly on the two day mass loadings.

Cloud condensation nucleus concentrations decreased sharply with decreasing supersaturation. Coincident with this was a decline in particle number concentration and a gradual decrease in the concentration of water soluble ions, both of which occurred with increasing particle size. Agreement between the numbers of cloud nuclei active at 0.1 to 0.2% supersaturation and the AN concentrations suggest that most of the particles, in the absence of a diurnal variation in AN, were larger than $\sim$0.1 μm.

The measured size distributions, expressed in a logarithmic form, can be approximated by a Junge power law function (Junge, 1963). The resulting slopes of this function vary between -3.0 and -3.4, which indicates similar particle volumes in equal log diameter classes over the size range 0.2–4.0 μm. This result is consistent with measurements of aerosol particles over continents. The size distributions obtained from measurements performed by Heintzenberg (1980) on the springtime Arctic aerosol showed a more pronounced accumulation of particles around 0.2–0.3 μm diameter than found here, although the total mass estimates are very similar. It is possible that the aerosol observed during this study had aged for a longer period, which might lead to this difference, but it is equally likely that measurement error is responsible. The mass and surface distributions from the period 19–21 February (Fig. 5) were slightly reduced in concentration and resemble the volume and surface distributions suggested by Jaenicke (1980) for a background aerosol.

A comparison of the size distribution determined from the Royco CCN measurements with measurements of the light-scattering coefficient highlights an

important discrepancy. A sample calculation of the light-scattering coefficient (Table 1) as derived from the above size distribution, for the period 19–21 February, produces a result which is approximately a factor of 2 below the measured scattering coefficient. The same calculation for the period 23–26 February is again a factor of 2 below the measured value. The discrepancy can be reduced by examination of the differential in the aerosol light-scattering coefficient between 22 and 23 February. During this time period the light-scattering signal increased by $\sim 2.6 \times 10^{-5}$ m^{-1} and the concentration of large particles increased by ~ 2.5 cm^{-3}. The latter increase corresponds to a calculated increase in b_{scat} of $\sim 1.8 \times 10^{-5}$ m^{-1}. This somewhat better agreement was also observed between the declines in the large particle concentration and in the light-scattering coefficient for 23–26 February, giving reason to suspect that the light-scattering signal may have had a component from other than aerosol and Rayleigh scattering. This may have resulted from a zero problem with the nephelometer or possibly from scattering by ice crystals. Other sources of error which hinder this comparison are optical absorption by the particles, weaknesses in the assumptions used in the particle scattering calculations, a Royco response function which may have been less sensitive to natural aerosol particles than the calibration particles, or an underestimation of the CCN concentrations. It is unlikely that the hygroscopicity of the particles influenced the discrepancies between the different measurements, because the relative humidity was usually <80% and the temperature difference between the sampling (indoor) and ambient environments was large enough to promote drying of the particles.

TABLE 1. Light-scattering coefficient calculation for size distribution in Fig. 4a.

Diameter (μm)	Q_{scat} (m = 1.5; λ = 0.5 μm)	ΔN (cm^{-3})	b_{scat}* ($\times 10^{10}$ cm^{-1})
0.20	0.3	13	12
0.25	0.8	20	79
0.30	1.7	10	120
0.35	2.1	5.0	100
0.40	2.6	3.0	98
0.45	3.1	1.8	89
0.50	3.4	1.5	100
0.55	3.8	0.90	81
0.60	4.0	0.60	68
0.65	4.1	0.40	54
0.70	4.2	0.55	89
0.80	4.0	0.39	78
0.90	3.9	0.23	57
1.0	2.8	0.22	55
1.2	2.0	0.16	36
1.4	2.1	0.09	29
1.6	3.0	0.05	30
1.8	2.8	0.03	21
2.0	2.4	0.03	23
2.5	2.5	0.03	37

* Total = 1.3×10^{-5} m^{-1}.

The concentrations of impacted aerosol particles measured under a light microscope are about a factor of 3 below the concentrations determined by the Royco. A low collection efficiency of the impactor may have been responsible for this result.

Analyses for the major water soluble ionic species composing the particulate mass (at both the remote and laboratory sites) indicated sulphate ($SO_4^=$) to have been the dominant anion and ammonium (NH_4^+) the dominant cation. Hydrogen ion was not measured directly. Mean concentrations of $SO_4^=$ and NH_4^+ for the period 19–21 February were 0.47 and 0.12 μg m^{-3}, respectively, and neither species was found in particles with an aerodynamic size > 2 μm. This $SO_4^=$ concentration is only slightly higher than the particulate sulphur results for a background aerosol obtained by Flyger *et al.* (1976). During 23–26 February, the average values for $SO_4^=$ and NH_4^+ were 3.0 and 0.65 μg m^{-3}, respectively, for particle sizes less than 2 μm. Above 2 μm diameter, 0.2 and 0.01 μg m^{-3} of $SO_4^=$ and NH_4^+ were measured, respectively. Molar concentrations of NH_4^+ and the other cations measured (Na^+, Mg^{++}, Ca^{++}) were insufficient to balance the molar values of $SO_4^=$ and NO_3^-, suggesting that the aerosol particles may have been quite acidic during this study (Hoff *et al.*, 1983).

A small sea-salt component as well as the low concentration of particles > 4 μm (Figs. 5 and 6) makes is unlikely that these air masses had any recent particle input from a maritime source. Prior to 22 February, Na^+ and Cl^- ions composed $\sim$35% of the water soluble mass, while after 22 February this ratio dropped to $\sim$14%. The lack of giant aerosol particles is attributed to gravitational settling and washout. Residence of the air masses over snow- and ice-covered terrain is hypothesized to have suppressed generation or re-entrainment of new particles in this portion of the size spectrum.

The distribution of the particulate water soluble mass parallels the Royco-generated surface distributions for both periods, suggesting that the formation of aerosol $SO_4^=$ was diffusion controlled either by gas-to-particle conversion and subsequent coagulation with existing aerosol, or by heterogeneous oxidation of SO_2, if the latter was rate-limited by the diffusion of SO_2. Heterogeneous oxidation may be more effective in winter environments because of higher relative humidities (Mezaros, 1968, 1978).

Comparison of the total of the ion concentrations with the total particulate mass (estimated from the Royco measurements) as shown in Figs. 5 and 6 indicates that during 19–21 February $\sim$35% of the aerosol particles less than 2 μm were water soluble. This ratio increased to $\sim$75% for collections made between 23 and 26 February. For particles larger than 2 μm, the ratios of water soluble mass to total particulate

mass were estimated to be ~15 and ~35% for the respective time periods. Light microscope determinations of the size distribution (Fig. 6) suggest that from 23 to 26 February the aerosol particles were composed essentially of water soluble materials. Visual observations of the filters showed slight darkening, indicating that some soot or other dark (possibly insoluble) material was present in the aerosol. Such darkening has been observed previously at this site by Barrie *et al.* (1981). Clay minerals might also have composed a portion of the aerosol. Although no Ca^{++} was detected, materials such as silicates have been observed in the submicron aerosol (Pitchford *et al.*, 1981) and have been found in the Arctic aerosol (Kumai and Frances, 1962; Shaw, 1983).

The visual range estimates may be compared against particle observations by making use of the Koschmieder relation

$$V = 3.9\sigma^{-1}, \quad (1)$$

where V is the visual range and σ is the extinction coefficient. This relation allows us to make a simple estimate of the visual range using optical extinction measurements. From 23 to 26 February the mean particle scattering coefficient determined with the nephelometer was 4.3×10^{-5} m^{-1}. This value is assumed to represent primarily submicron aerosol particle scattering; however, as discussed before it may contain a component due to ice crystals. Accounting for Rayleigh scattering at −30°C and 1000 mb, the total scattering coefficient is estimated to be 6.4×10^{-5} m^{-1}. This produces a visibility estimate of ~60 km based on (1). By comparison, direct estimates of visibility during the study varied between 10 and 60 km when no precipitation was visible.

The relative contribution by suspended ice crystals to the reduction in visibility can be estimated from Fig. 7. The crystal area per unit volume in general is comparable to the scattering estimates for the smaller aerosol particles and molecules. Although crystal orientation may tend to reduce the scattering ability of the crystals in any given direction, factors such as impaction losses, which lead to an underestimation of crystal concentration, and the efficiency of scattering, should increase the scattering of light by ice crystals. The addition of an ice crystal component to the total scattering coefficient would improve the comparison between observation and calculation of the visual range. Thus, suspended ice crystals appear to have been an important, if not dominant, fraction of the light scattering aerosol.

It was hoped to examine the issue of aerosol transport by means of aircraft observations. Unfortunately this platform was available only for one day (26 February). Results from that day (Fig. 9) showed a large vertical gradient in AN concentration with the surface layer acting as a source of small particles. A temperature profile in ascent (Fig. 9c) showed the surface mixed layer to be about 100 m thick. The AN profile showed a decrease in concentration with altitude. The simple diffusion formula

$$N(Z) = N(0) \exp(-Z/H), \quad (2)$$

where H is the mixing height and Z is the altitude, is plotted in Fig. 9c as a dashed line where $N(0) = 1300$ cm^{-3} and $H = 100$ m. The agreement between this curve and the AN measurements is generally good and the deviation above 200 m is explainable by both instrument error and the presence of large particles. The vertical distribution thus suggests that these nuclei were transported aloft by diffusion. In contrast, Flyger *et al.* (1976) have found small nuclei production at 3 km altitude in the summertime. The concentration of large particles, as represented by the light-scattering coefficient, was uniform throughout the lower troposphere (up to ~1 km) contained by the surface inversion. The relatively particle-free air above this (Figs. 9a and b), associated with southerly winds, suggests that there was little relation between the two layers. Physical characteristics of the surface aerosol indicate that most of the large particles were present as a suspension for several days prior to the observations.

The sharp increase in the particle concentration between 22 and 23 February, illustrated in Fig. 3, would appear to mark some horizontal transport phenomenon. Chemical and physical analyses of the aerosol observed prior to 22 February suggest that concentrations were very close to background levels. Analyses of upper-air data from Hall Beach showed a significant influx of warm air between about 800 and 900 mb beginning on 18 February and intensifying over 21–22 February. Late on 22 February and early on 23 February the temperature decreased by several degrees from the surface up to ~800 mb. A five-day back trajectory (Hoff *et al.*, 1983) and chart analyses up to 850 mb show that the air arriving at Igloolik on the 23, 24 and part of the 25 February had passed over the polar ice cap northwest of Igloolik, a result of a high pressure system to the west. It is possible that the upper warm air influx over 18–22 February had subsided and with it carried an increase in particle concentrations. However, this seems unlikely because the subsidence motion does not appear to have reached the surface (the inversion at ~1 km was maintained from 19 February) and the vertical profile for 26 February suggests that warm air aloft possessed depressed concentrations relative to the surface. Based on these findings, the elevated particulate loadings are believed to have accompanied the advection of northern polar air near the surface. Whether the observed aerosol existed in the surface layer from its source to our observation point is not speculated upon, but it does appear to have been anthropogenic in origin. This is supported by detailed chemical analysis (Hoff *et al.*, 1983).

6. Conclusions

Observations of total aerosol particle concentration, size distributions, cloud nuclei spectra, aerosol light scattering coefficient, ice crystal concentrations and visual range estimates have been evaluated for a site at Igloolik, Northwest Territories. The vertical variations of Aitken nucleus concentrations, light-scattering coefficient and temperature were examined on one day. The results of this study lead to the following conclusions which may be generalized for the Arctic aerosol in so much as the observations were free from local influences but must be considered more specific because of the short observation period:

1) A peak in the total number concentration of aerosol particles was observed frequently near midday, but this diurnal variation was confined to small nuclei (<0.1 μm) and seems to have little short-term (days) effect on the large or giant particle mass.

2) The water soluble particles of the aerosol possessed a much lower volume mean diameter than that of the total aerosol particle mass (<10 μm) calculated from measurements with the Royco. The distribution with particle size of the water soluble ions paralleled the surface distribution extracted from the Royco measurements. The dominant water soluble ion was $SO_4^=$.

3) Polar air advected from the northwest brought with it a large increase in particle mass and a relatively larger increase in the concentration of $SO_4^=$. Virtually all of the submicron particles were composed of some compound of sulphate.

4) Throughout the period 19–26 February the aerosol possessed the characteristics of having been well-aged. Prior to 22 February, particle concentrations approached background levels, while after 22 February they had been influenced by anthropogenic sources.

5) During one day (26 February) the Aitken nucleus concentrations were found to decrease with height above the surface in a manner indicative of diffusive transport. This transport of small nuclei was independent of the light-scattering (large) aerosol particles, suggesting that these different particle classes had different sources and probably different residence times.

6) Ice crystals (>10 μm) were found to be potentially more important than the submicron aerosol particles to the scattering of visible light.

Acknowledgments. One of us (WRL) acknowledges the Natural Sciences and Engineering Research Council of Canada Visiting Fellowship program.

We are indebted to Dr. Andy Rode, Head of the Eastern Arctic Research Laboratory in Igloolik, and George Qualuat who were very gracious and accommodating hosts during the study.

We thank Professor W. J. Megaw of York University, Toronto, for providing aerosol laboratory facilities, Dr. J. Hudson of the Desert Research Institute, Reno, Nevada, for providing the calibration of the Royco counter, and P. Fellin of the Atmospheric Environment Service who performed the ion analyses.

REFERENCES

Barrie, L. A., R. M. Hoff and S. M. Daggupaty, 1981: The influence of midlatitudinal pollution sources on haze in the Canadian Arctic. *Atmos. Environ.*, **15,** 1407–1419.

Flyger, H., N. Z. Heidam, K. Hansen, W. J. Megaw, E. G. Walther and A. W. Hogan, 1976: The background level of the summer tropospheric aerosol, sulphur dioxide and ozone over Greenland and the North Atlantic Ocean. *J. Aerosol Sci.*, **7,** 103–140.

Heintzenberg, J., 1980: Particle size distribution and optical properties of Arctic haze. *Tellus,* **32,** 251–260.

Hoff, R. M., W. R. Leaitch, P. Fellin and L. A. Barrie, 1983: Mass size distributions of chemical constituents of the winter Arctic aerosol. *J. Geophys. Res.*, **88,** 10 947–10 956.

Hogan, A. W., 1977: A simplified aerosol coagulation model. *J. Air Pollut. Control Assoc.*, **27,** 759–762.

——, W. Winter and G. Gardner, 1975: A portable aerosol detector of high sensitivity. *J. Appl. Meteor.*, **14,** 39–45.

——, S. C. Barnard and W. Winters, 1982: Aerosol minima. *Geophys. Res. Lett.*, **9,** 1251–1254.

Jaenicke, R., 1980: Atmospheric aerosols and global climate. *J. Aerosol Sci.*, **11,** 577–588.

Junge, C. E., 1963: *Air Chemistry and Radioactivity.* Academic Press, 382 pp.

Kumai, M., and K. E. Francis, 1962: Nuclei in snow and ice crystals on the Greenland ice cap under natural and artificially stimulated conditions. *J. Atmos. Sci.*, **19,** 474–481.

Leaitch, R., and W. J. Megaw, 1982a: The diffusion tube; a cloud condensation nucleus counter for use below 0.3% supersaturation. *J. Aerosol. Sci.*, **13,** 297–319.

——, and ——, 1982b: Investigation of atmospheric CCN using the diffusion tube. *Idojaras,* **86,** 217–225.

May, K. R., 1945: The cascade impactor: An instrument for sampling coarse aerosols. *J. Sci. Instrum.*, **22,** 187–195.

Megaw, W. J., and H. Flyger, 1973: Measurement of the background atmospheric aerosol. *J. Aerosol. Sci.*, **4,** 179–181.

Mezaros, A., 1978: On the concentration and size distribution of atmospheric sulphate particles under rural conditions. *Atmos. Environ.*, **12,** 2425–2428.

Mezaros, E., 1968: On the size distribution of water soluble materials. *Tellus,* **20,** 443–448.

Mitchell, M., 1957: Visual range in the polar regions with particular reference to the Alaskan Arctic. *J. Atmos. Terr. Phys.* (Spec. Suppl.), 195–211.

Pitchford, M., R. G. Flocchini, R. G. Draftz, T. A. Cahill, L. L. Ashbaugh and R. A. Eldred, 1981: Silicon in submicron particles in the Southwest. *Atmos. Environ.*, **15,** 321–333.

Radke, L. A. F., P. V. Hobbs and J. E. Pinnons, 1976: Observations of cloud and condensation nuclei, sodium-containing particles, ice nuclei and the light-scattering coefficient near Barrow, Alaska. *J. Appl. Meteor.*, **15,** 982–995.

Rahn, K. A., 1982: Elemental tracers for source regions of Arctic pollution aerosol. *Idojaras,* **86,** 1–14.

——, R. D. Borys and G. E. Shaw, 1977: The Asian source of the Arctic haze bands. *Nature,* **268,** 713–715.

Rich, T. A., 1955: Photo electric nucleus counter with size discrimination. *Geofis. Pura Appl.*, **31,** 60–65.

Schaefer, V. A., 1946: The production of ice crystals in a cloud of supercooled water droplets. *Science,* **104,** 457.

Shaw, G. E., 1975: The vertical distribution of tropospheric aerosol at Barrow, Alaska. *Tellus,* **27,** 39–49.

——, 1983: X-ray spectrometry of polar aerosols. *Atmos. Environ.*, **17,** 329–339.

——, and K. Stamnes, 1980: Arctic haze: Perturbation of the polar radiation budget. *Ann. N.Y. Acad. Sci.*, **338,** 533–539.